IEICE Electronics Express, Vol.18, No.1, 1–4

LETTER

Optical high-gain leaky-wave antenna by using a waffle-iron waveguide

Shunichi Kaneoka[1, a)], **Wataru Iida**[1], **Hiroshi Hashiguchi**[1], **Toshihiko Baba**[1], **and Hiroyuki Arai**[1]

Abstract This paper presents a comparison of optical leaky-waveguide antennas, i.e., grating waveguide (GWG), waffle waveguide (WWG), and waffle-iron waveguide (WIWG), using both simulations and measurements. WIWG radiates a narrow beam that is tilted by sweeping the incident wavelength, and it possesses a higher antenna gain than GWG and WWG under the same fabrication condition. The reason is due to a slight difference in the effective index along the longitudinal sections, which provides a large aperture size for high antenna gain. We simulate the antenna characteristics and experimentally confirm the high antenna gain.

Keywords: optical antenna, leaky waveguide, grating waveguide, waffle waveguide, waffle-iron waveguide

Classification: Integrated optoelectronics (lasers and optoelectronic devices, silicon photonics, planar lightwave circuits, polymer optical circuits, etc.)

1. Introduction

High-speed and large-capacity data transmission will be required in future wireless-communication systems. The carrier frequency used in optical wireless communication is higher than that in the terahertz band, which can enable us to meet the demand beyond 5G communication systems [1, 2, 3, 4, 5]. In addition, the antenna for optical wireless communication can be downsized because of the very short wavelength in the optical bands, and silicon photonics would be suitable for manufacturing such a small antenna for mass production at low cost [6, 7, 8, 9, 10, 11, 12, 13, 14, 15, 16, 17, 18]. Considering the communication environment, the antenna gain is so high enough to communicate with long distance. However, the high gain means the small beamwidth which is inconvenient for covering the wide communication area. For this reason, the optical waveguide such as grating couplers and optical phased array is proposed [19, 20, 21, 22, 23, 24, 25, 26, 27]. This waveguide can control the direction of radiation beam, so it ensure high gain and wide communication area by beamforming. These waveguides are called optical leaky-wave antenna (OLWA). The waffle-iron waveguide (WIWG), which is one of the OLWA, is proposed to enhance the antenna gain during the simulation [28]. Then, we confirm its performance by comparing it with other waveguides using effective index and measurement.

[1] Graduate School of Engineering Science, Yokohama National University, 79–5 Tokiwadai, Hodogayaku, Yokohama-city, Kanagawa 240–8501, Japan

[a)] kaneoka-shunichi-zr@ynu.jp

DOI: 10.1587/elex.17.20200411
Received December 1, 2020
Accepted December 9, 2020
Publicized December 22, 2020
Copyedited January 10, 2021

The present study shows the geometry of each waveguide and discusses the difference in their characteristics using an effective index, as presented in Section 2. The simulation and experimental demonstration of the WIWG is described in Section 3 to show its high antenna-gain performance. The conclusion is provided Section 4.

2. The effect of WIWG

We fabricate these waveguides using the silicon photonics technology, which can fabricate optical components with low cost using a mass-fabrication process. Fig. 1 shows the geometries and design parameters of the conventional grating waveguide (GWG), waffle waveguide (WWG), and WIWG. These waveguides are fabricated in a Si layer in which the height on the silica substrate is 0.21 μm for a single-mode propagation of light, as shown in Fig. 2(a). The indexes of silicon and silica are 3.45 and 1.45, respectively. GWG has periodical grooves on the surface, as shown in Fig. 2(b). These periodic grooves provide index perturbation and excite a leaky wave along the z-axis. The direction of the leaky wave is adjusted by Λ_y, and we set it to 0.57 μm and use a duty cycle of 0.5 to radiate the wave toward the zenith at $\lambda = 1.55\,\mu$m. Waveguide length L is a product of period Λ_y and number of periods N_y. We set $N_y = 200$, waveguide width $W = 10\,\mu$m, and etching depth $d = 0.01$ to

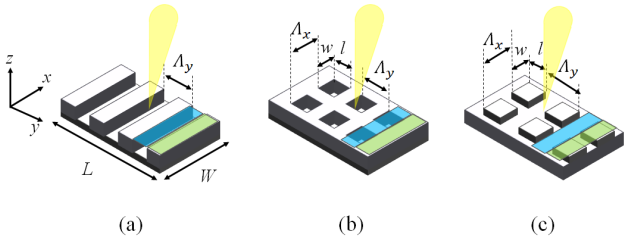

Fig. 1 Bird's eye view of each waveguide, green area: region A, blue area: region B, (a) GWG, (b) WWG, (c) WIWG, $W = 10\,\mu$m, $L = 114\,\mu$m, $w = 0.24\,\mu$m, $l = 0.29\,\mu$m, $\Lambda_x = 0.48\,\mu$m, $\Lambda_y = 0.57\,\mu$m.

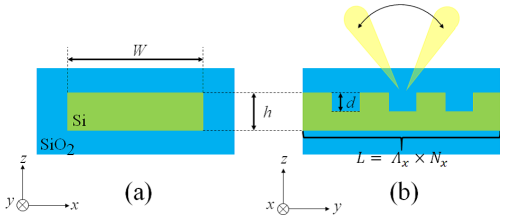

Fig. 2 Structure of leaky waveguide, (a) yz-plane view, (b) zx-plane view, $W = 10\,\mu$m, $h = 0.21\,\mu$m, $d = 0.07\,\mu$m, $\Lambda_x = 0.48\,\mu$m, $\Lambda_y = 0.57\,\mu$m, $N_x = 200$.

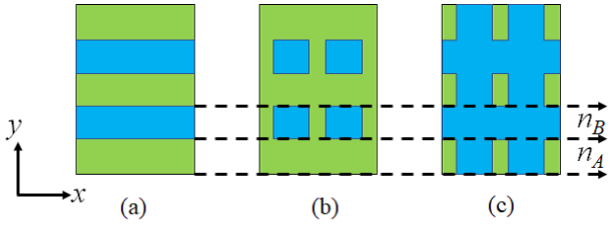

Fig. 3 Two regions on surface of each waveguide for effective index, (a) GWG, (b) WWG, (c) WIWG.

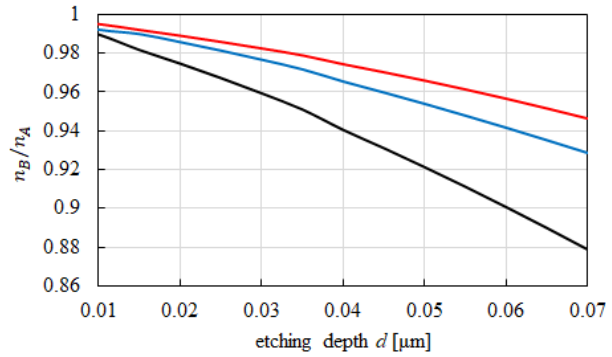

Fig. 4 The difference of effective index between region A and B, black: GWG, blue: WWG, red: WIWG.

0.07 μm to compare the effect of the structures. To reduce the leaky-wave radiation in a unit period, we need to reduce the index difference (perturbation) between the condition without grooves for n_A and that with grooves for n_B, as shown in Fig. 3(a). The index difference is reduced by employing shallow etch grating. However, $d = 0.01\,\mu$m is the minimum etch deep because of fabrication constraint. We propose WWG to reduce the index difference. WWG has a rectangular etching array on the Si layer and reduces the index difference between n_A and n_B, as shown in Fig. 3(b). A part of the silicon in Region B is increased by the waffle structure; thus, the effective index of n_B approaches n_A. The WWG parameters with period Λ_y, length L, and width W are set to be the same as the GWG parameters. Period Λ_x, the duty cycle, and number of periods N_x in the y direction are set to 0.48, 0.5, and 20, respectively, to further reduce the index difference. WIWG with a rectangular etching array on the waveguide surface, which has an inverse structure as that of WWG, is also proposed [28]. A part of silica in Region A is increased by the waffle-iron structure. Thus, the difference between effective indexes n_A and n_B becomes small, as shown in Fig. 3(c). Figure 4 shows the comparison of the index differences in Regions A and B as a function of etch depth d. The index difference is defined as n_B/n_A and becomes small for a shallow etch depth. WIWG has the smallest structure among the three waveguides. Therefore, WIWG exhibits the smallest perturbation, resulting in good aperture efficiency and high directive gain [29].

3. Comparison of waveguide characteristics

This section presents the comparison of the characteristics of the three waveguides using simulation and experiment. First, we show the transmission characteristics to verify that WIWG has the longest effective length and confirm its gain

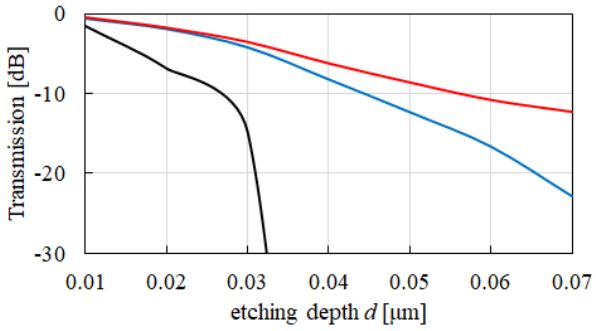

Fig. 5 Transmission characteristics over etching depth at 193.75 THz, black: GWG, blue: WWG, red: WIWG.

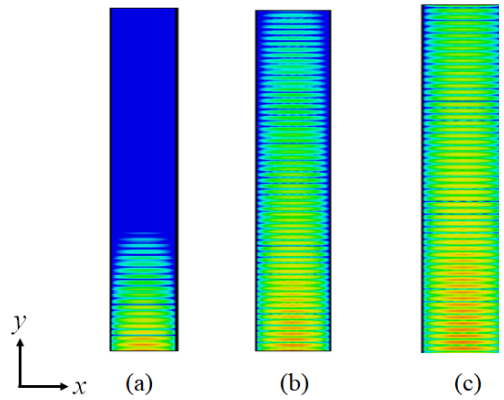

Fig. 6 Electric field distribution as 0.07 μm etching, (a) GWG, (b) WWG, (c) WIWG.

enhancement by the experiment.

Figure 5 shows the result of the transmission characteristics when the carrier frequency is 193.75 THz. In the case of shallow etching, the characteristics are close to one another because the differences in the effective index are almost the same, as shown in Fig. 4. However, they are apparently different from one another as the etching depth increases. This result corresponds to that shown in Fig. 5 and demonstrates that WIWG has the smallest attenuation. Its effective antenna length is also the longest. Figure 6 shows the electric-field distribution of each waveguide. The field intensity is attenuated along the waveguide because light is radiated from its surface. Therefore, we confirm that WIWG has the most effective antenna that can realize gain enhancement, as presented in Section 2.

Then, we describe the performance evaluation of each waveguide through experiment. The experimental system to measure the radiation power on each waveguide surface is shown in Fig. 7. First, an optical laser illuminates the waveguide end through using a tunable laser with a wavelength of 1.55 μm, which is the wavelength band used in far-infrared communication. The scattered power from the waveguide is monitored using an Indium gallium arsenide (InGaAs) camera installed above the waveguide. The radiated power is measured by a power meter while the camera is moved at certain fixed intervals, 0.5 μm. Because this power includes the propagation and coupling loss of the optical fiber, the measurement results are normalized to exclude the coupling loss. To enhance the gain, we use the fabricated chip with 0.01 μm etching depth and 1000 periods along the longitu-

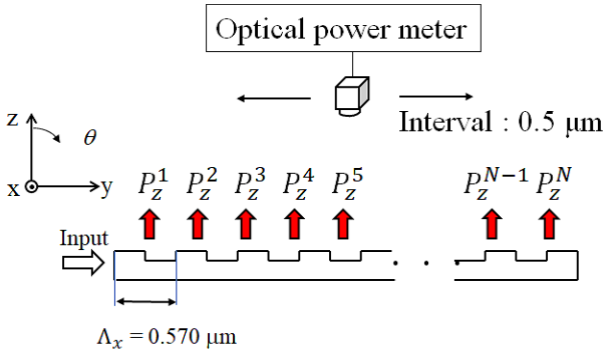

Fig. 7 Measurement setup for power distribution.

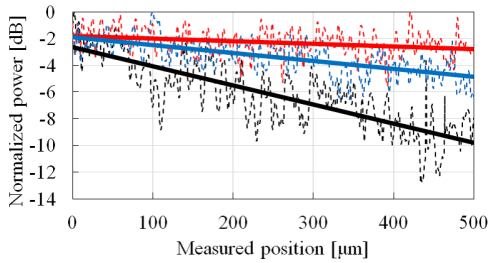

Fig. 8 Radiation power distribution, black: GWG, blue: WWG, red: WIWG, dotted lines are measurements and straight lines are approximations.

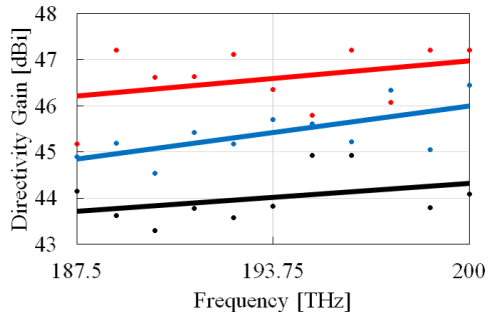

Fig. 9 Experimental directivity gain, black: GWG, blue: WWG, red: WIWG, dotted lines are measurements and straight lines are approximations.

dinal direction. Figure 8 shows the results of the measured radiated power. From this figure, WIWG exhibits the smallest attenuation coefficient, and GWG and WWG have larger attenuation. In other words, WIWG has the largest effective aperture size, resulting in the highest antenna gain theoretically shown by the following equation:

$$G = \left(\frac{\pi D}{\lambda}\right)^2 \eta \tag{1}$$

where D and η are aperture size and aperture efficiency, respectively. These parameters are the indicator of excitation for the reflector antenna such as horn and parabolic reflector antenna [30]. Finally, we derive the directivity gain using this measurement. In this study, we utilize the beamwidth to estimate the directivity gain. The directivity gain is expressed by the following equation:

$$G_{est} = 10\log_{10}\left(\frac{52525}{\theta\varphi}\right) \tag{2}$$

where θ and φ are the beamwidths in the two orthogonal planes [31]. Figure 9 shows the results using this estimation method. Because the estimation is performed using the values obtained in the experiment, data scattering occurs due to manufacturing errors, but WIWG still shows the highest directivity gain.

4. Conclusion

In this paper, we propose a high-gain antenna suitable for a base-station antenna used in optical wireless communication. In conclusion, WIWG is revealed to be a useful antenna. This high-gain antenna is indispensable because optical wireless communication incurs large losses.

References

[1] J.M. Kahn and J.R. Barry: "Wireless infrared communications," Proc. IEEE **85** (1997) 265 (DOI: 10.1109/5.554222).
[2] H.S. Chung, *et al.*: "Optical access technologies for 5G mobile communication networks," 2017 IEEE Photonics Society Summer Topical Meeting Series (SUM) (2017) 39 (DOI: 10.1109/PHOSST.2017.8012640).
[3] K. Kim, *et al.*: "High speed and low latency passive optical network for 5G wireless systems," J. Lightw. Technol. **37** (2019) 2873 (DOI: 10.1109/JLT.2018.2866805).
[4] J.P. Turkiewicz: "Optical transmission technologies for 5G networks," 2019 21st International Conference on Transparent Optical Networks (ICTON) (2019) 1 (DOI: 10.1109/ICTON.2019.8840559).
[5] W. Boubakri, *et al.*: "An optical wireless communication based 5G architecture to enable smart city applications," 2018 20th International Conference on Transparent Optical Networks (ICTON) (2018) 1 (DOI: 10.1109/ICTON.2018.8473657).
[6] T. Baba and K. Yamada: "Progress in silicon photonics and recent activities in Asia," OECC 2010 Technical Digest (2010) 10.
[7] K. Ohashi, *et al.*: "A silicon photonics approach for the nanotechnology era," 2007 IEEE International Electron Devices Meeting (2007) 787 (DOI: 10.1109/IEDM.2007.4419065).
[8] K. Yamada: "Advanced silicon photonics for post-Moore era," 42nd European Conference on Optical Communication (2016) 1.
[9] W. Zhang and J. Yao: "Silicon-based integrated microwave photonics," IEEE J. Quantum Electron. **52** (2016) 0600412 (DOI: 10.1109/JQE.2015.2501639).
[10] E. Ryckeboer, *et al.*: "Spectroscopic sensing and applications in Silicon Photonics," 2017 IEEE 14th International Conference on Group IV Photonics (GFP) (2017) 81 (DOI: 10.1109/GROUP4.2017.8082206).
[11] W. Withayachumnankul, *et al.*: "Evolution of rod antennas for integrated terahertz photonics," 2018 43rd International Conference on Infrared, Millimeter, and Terahertz Waves (IRMMW-THz) (2018) 1 (DOI: 10.1109/IRMMW-THz.2018.8509906).
[12] F.J. Díaz-Fernández, *et al.*: "Characterisation of on-chip wireless interconnects based on silicon nanoantennas via near-field scanning optical microscopy," IET Optoelectronics **13** (2019) 72 (DOI: 10.1049/iet-opt.2018.5071).
[13] Z. Yao, *et al.*: "Integrated silicon photonic microresonators: emerging technologies," IEEE J. Sel. Topics Quantum Electron. **24** (2018) 5900324 (DOI: 10.1109/JSTQE.2018.2846047).
[14] R. Soref: "The past, present, and future of silicon photonics," IEEE J. Sel. Topics Quantum Electron. **12** (2006) 1678 (DOI: 10.1109/JSTQE.2006.883151).
[15] M. Hochberg, *et al.*: "Silicon photonics: the next fabless semiconductor industry," IEEE Solid-State Circuits Mag. **5** (2013) 48 (DOI: 10.1109/MSSC.2012.2232791).
[16] P. Dumon, *et al.*: "Towards foundry approach for silicon photonics: silicon photonics platform ePIXfab," Electronics Letters **45** (2009) 581 (DOI: 10.1049/el.2009.1353).
[17] T. Baba: "Photonic crystals and silicon photonics," 2008 International Nano-Optoelectronics Workshop (2008) 56 (DOI: 10.1109/INOW.2008.4634438).

[18] T. Baba, *et al.*: "Large delay-bandwidth product and tuning of slow light pulse in photonic crystal coupled waveguide," Opt. Express **16** (2008) 9245 (DOI: 10.1364/OE.16.009245).
[19] K. Van Acoleyen, *et al.*: "Off-chip beam steering with a one-dimensional optical phased array on silicon-on-insulator," Opt. Lett. **34** (2009) 1477 (DOI: 10.1364/OL.34.001477).
[20] R.M. Emmons and D.G. Hall: "Buried-oxide silicon-on-insulator structures. II. Waveguide grating couplers," IEEE J. Quantum Electron. **28** (1992) 164 (DOI: 10.1109/3.119511).
[21] J.T. Boyd and D.B. Anderson: "Effect of waveguide optical scattering on the integrated optical spectrum analyzer dynamic range," IEEE J. Quantum Electron. **14** (1978) 437 (DOI: 10.1109/JQE.1978.1069811).
[22] S. Zhu and G.-Q. Lo: "Design of integrated optical beam steerer based on cascaded ring resonator," 2015 IEEE International Conference on Electron Devices and Solid-State Circuits (EDSSC) (2015) 33 (DOI: 10.1109/EDSSC.2015.7285042).
[23] S. Zhu, *et al.*: "A large-angle single-wavelength optical beam steerer based on cascaded ring resonator," 2016 International Conference on Optical MEMS and Nanophotonics (OMN) (2016) 1 (DOI: 10.1109/OMN.2016.7565817).
[24] C. Mekhiel and X. Fernando: "Monolithic silicon-on-insulator optical beam steering with phase locking heterodyne feedback," 2017 IEEE 28th Annual International Symposium on Personal, Indoor, and Mobile Radio Communications (PIMRC) (2017) 1 (DOI: 10.1109/PIMRC.2017.8292184).
[25] Z. Du, *et al.*: "Integrated wavelength beam emitter on silicon for two-dimensional optical scanning," IEEE Photon. J. **11** (2019) 6603710 (DOI: 10.1109/JPHOT.2019.2943641).
[26] S. Ura, *et al.*: "Vertically stacked and directionally coupled cavity-resonator-integrated grating couplers for integrated-optic beam steering," 2019 IEEE 69th Electronic Components and Technology Conference (ECTC) (2019) 556 (DOI: 10.1109/ECTC.2019.00090).
[27] K. Kondo, *et al.*: "Fan-beam steering device using a photonic crystal slow-light waveguide with surface diffraction grating," Opt. Lett. **42** (2017) 4990 (DOI: 10.1364/OL.42.004990).
[28] H. Hashiguchi, *et al.*: "Optical leaky waveguide antenna using shallow etched circular waffled waveguide," 2017 IEEE International Symposium on Antennas and Propagation & USNC/URSI National Radio Science Meeting (2017) 1275 (DOI: 10.1109/APUSNCURSINRSM.2017.8072680).
[29] W.V. McLevige, *et al.*: "New waveguide structures for millimeter-wave and optical integrated circuits," IEEE Trans. Microw. Theory Techn. **23** (1975) 788 (DOI: 10.1109/TMTT.1975.1128684).
[30] H. Hashiguchi: "A study on antenna gain enhancement and excitation method of optical leaky wave antenna," Ph. D. Dissertation, Yokohama National University (2019).
[31] M. Thereza: *Handbook of Antennas for EMC* (Artech House Publishers, 1995) 26.